



Poly(Azomethine-urethane)-based Fluorescent Chemosensor for the Detection of Cr³⁺ Cations in Different Water Samples

Musa Kamaci¹

Received: 1 August 2022 / Accepted: 29 September 2022 / Published online: 12 October 2022
© The Author(s), under exclusive licence to Springer Science+Business Media, LLC, part of Springer Nature 2022

Abstract

A highly selective, and effective poly(azomethine-urethane)-based chemosensor (HIMA) was prepared, and it used as a fluorescent sensor for the detection of Cr³⁺ cations in different solutions. The HIMA was prepared in two-step reactions by using hexamethylene diisocyanate, 2,4-dihydroxy benzaldehyde, and 2-aminophenol. The sensitivity and selectivity of the fluorescent probe were tested in the presence of different metal ions. The obtained findings indicated that the chemosensor exhibited a quenching effect against the only Cr³⁺ ion. The limit of detection (LOD) and limit of quantitation (LOQ) of the chemosensor HIMA were calculated as 7.98×10^{-7} M, and 2.42×10^{-6} M, respectively. In addition, the binding constant (K_a) of the chemosensor was calculated as 5.31×10^5 M⁻¹.

Keywords Fluorescence · Chromium · Chemosensor · Polyurethane · Quenching

Introduction

Chromium is one of the important heavy elements in the focus of wastewater treatment due to its wide range of applications such as chromate production, electroplating, metal mining, textile industry, and wood corrosion resistance [1–3]. It is generally found as trivalent (Cr³⁺), and hexavalent (Cr⁶⁺) cations in aqueous media due to the stable oxidation states [4]. They can be found as different compounds such as Cr(OH)₃, CrO₄²⁻, etc. depending on the temperature and pH value of the water, the reduction–oxidation potential, and the concentration of chromium [5, 6]. Among these species, Cr³⁺ is an essential element in daily human and animal nutrition, and it has a non-toxic behavior [7]. Besides, chromium plays an important role such as enzyme and RNA formation, accelerating blood coagulation, increasing β-glucuronidase activity, secretion of hormones and some vitamins, increasing immunity, feed intake, and energy efficiency in animals [8, 9].

Polyurethanes (PUs), which contain the urethane group in the main chain as their characteristic properties, are attracting more and more attention due to their structural flexibility, ion

transportability, mechanical properties, thermal conductivity, flexibility, chemical and wear resistance [10, 11]. They have also exhibited superior compatibility with other polymers and inorganic materials, and poly(azomethine-urethane)s derivatives of polyurethane have been also reported in the literature due to these properties [12, 13]. To the best of our knowledge, there are very few studies reported in the literature regarding the development of poly(azomethine-urethanes) as fluorescence sensors for the detection of cations or analytes. Among these studies, they were used to detection of Mn²⁺ [14], Cd²⁺ [15], Zn²⁺ [16, 17], Cu²⁺ [18], Fe³⁺ [19, 20], and DNA [21] and PAMU-based fluorescence sensor for the detection of Cr³⁺ cations with good selectivity, and sensitivity has not been reported in the literature yet.

In the present paper, a poly(azomethine-urethane) (PAMU)-based fluorescent sensor was developed for the determination of Cr³⁺ cations in different solutions. For this purpose, PAMU was synthesized by two-step polymerization reactions. In the first reaction, polyurethane was prepared via copolymerization reaction of hexamethylene diisocyanate (HDI) with 2,4-dihydroxy benzaldehyde (HBA), and then the poly(azomethine-urethane) was obtained by the grafting of 2-aminophenol into the prepared pre-polymer. The fluorescence sensing behavior of the fluorescent chemosensor was tested in the presence of different cations such as Al³⁺, Ba²⁺, Cd²⁺, Co²⁺, Cr³⁺, Fe³⁺, K⁺, Li⁺, Mn²⁺, Ni²⁺, Pb²⁺, Zn²⁺, and Zr⁴⁺. According to the fluorescence measurements, the sensor responded as a quenching effect toward

✉ Musa Kamaci
mkamaci@pirireis.edu.tr

¹ Piri Reis University, 34940 Tuzla, Istanbul, Turkey

Cr(III) ions, and it has a good potential application for the detection of Cr(III) ions with high sensitivity and selectivity in different water samples.

Materials and Methods

Reagents

2-Aminophenol (2-AP), 2,4-dihydroxy benzaldehyde (HBA), hexamethylene diisocyanate (HDI), tetrahydrofuran (THF), dimethyl sulfoxide (DMSO), chloride salts of aluminum (III), barium (II), cadmium (II), chromium (III), cobalt (II), iron (III), nickel (II), potassium (I), and zirconium (IV), nitrate salts of lead (II), lithium (I), manganese (II), and zinc (II), and ethylenediaminetetraacetic acid (EDTA) were supplied as commercially from Sigma Aldrich, and they were used without any purification.

Preparation of the Chemosensor (HIMA)

The chemosensor ((*E*)-4-(((2-hydroxyphenyl)imino)methyl)-3-methoxyphenyl (6-acetamidohexyl)carbamate, HIMA) was prepared in two steps as in the previous paper (Fig. 1) [22]:

In the first step, the prepolymer was prepared by the copolymerization reaction of HBA (0.276 g, 2 mmol) and HDI (0.336 g, 2 mmol) in THF under Argon atmosphere for 24 h around 70 °C. In the last step, the chemosensor was obtained by the grafting of 2-AP (0.218 g, 2 mmol) into the preformed prepolymer (0.615 g, 2 mmol) in DMF/MeOH mixture (1:3; v:v) at 60 °C for 3 h.

Yield 82% for prepolymer, 85% for HIMA.

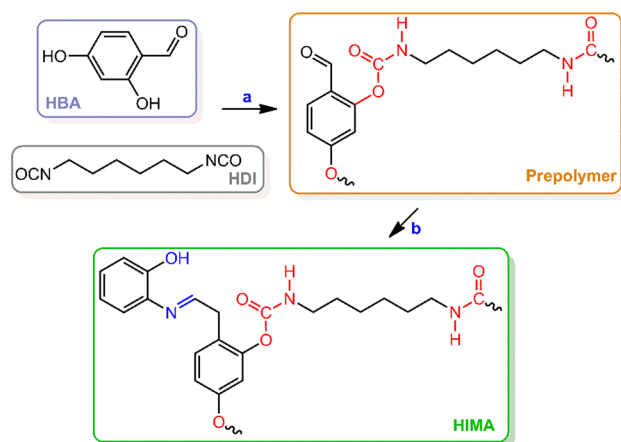


Fig. 1 Synthesis of the fluorescent probe (HIMA) (Reaction conditions; a: THF, reflux, 6 h, Ar atmosphere, and 70 °C; b: THF/MeOH mixture (1:3; v:v), reflux, 3 h, 2-aminophenol (2-AP), and 60 °C)

FT-IR (cm^{-1} , ν) 3321 (urethane –NH), 2936, 2861 (aliphatic –CH), 1705 (–CHO), and 1666 (urethane –C=O) for **prepolymer**, and 3320 (urethane –NH), 2932, 2858 (aliphatic –CH), 1645 (urethane –C=O), and 1588 (–N=CH) for **HIMA**.

$^1\text{H-NMR}$ (400 MHz, DMSO- d_6 , δ) 10.93 (–CHO), 7.90 (Ar–H), 7.67 (Ar–H), 7.65 (Ar–H), 6.76 (urethane –NH), 3.51 (Al–CH), 3.05 (Al–CH), and 1.33 (Al–CH) for **prepolymer**, and 9.83 (–OH), 7.86 (–N=CH), 6.93 (Al–CH), 6.71 (Al–CH), 6.79 (Al–CH), 6.77 (Al–CH), 6.73 (Al–CH), 6.68 (urethane –NH), 2.85 (Al–CH), 2.53 (Al–CH) and 1.35 (Al–CH) for **HIMA**.

GPC $M_n = 3300$ Da, $M_w = 4700$ Da, and PDI = 1.424 for **prepolymer**, and $M_n = 18300$ Da, $M_w = 25500$ Da, and PDI = 1.393 for **HIMA**.

Instruments

The polymer and fluorescent probe (HIMA) were characterized using FT-IR (Perkin-Elmer Spectrum Two Fourier Transform-Infrared Spectrometer), $^1\text{H-NMR}$ (Bruker AC FT-NMR 400 MHz Spectrometer), GPC (Shimadzu Gel Permeation Chromatography, eluent: DMF, standard: polystyrene) techniques.

Preparation of the Stock Solutions

A 24 μM stock solution of HIMA (0.061 g) was prepared in 100 mL DMF/deionized water (1:2; v:v) mixture. The aqueous stock solutions of metal cations (72 μM) such as Al^{3+} , Ba^{2+} , Cd^{2+} , Co^{2+} , Cr^{3+} , Fe^{3+} , K^+ , Li^+ , Mn^{2+} , Ni^{2+} , Pb^{2+} , Zn^{2+} , and Zr^{4+} were prepared in 10 mL deionized water by using their chloride or nitrate salts.

Optical Measurements

Absorption spectra of HIMA in the presence or absence of Cr^{3+} were measured using a Perkin-Elmer UV–Vis spectrophotometer between 250 and 800 nm. All fluorescence measurements were carried out by using a Perkin-Elmer LS 55 fluorescence spectrophotometer in the range from 500 to 800 nm in DMF/distilled water (1:2; v:v) mixture. Excitation and slit width were adjusted as 497 and 5 nm, respectively. In the tested absorption and fluorescence measurements solutions, the molar ratio of the HIMA and metal cations was 1:2 (v:v).

Results and Discussion

Absorption Measurements

Normalized absorption spectra of HIMA in the presence and absence of chromium (Cr^{3+}) solution were given in Fig. 2.

As can be seen in Fig. 2, the free HIMA chemosensor exhibited two absorbance bands at 347 and 423 nm due to $\pi \rightarrow \pi^*$, and $n \rightarrow \pi^*$ transitions, respectively [23, 24]. These transition bands were also recorded at 376, and 448 nm in the solution of the HIMA when added to Cr^{3+} cations, respectively. These results showed that the mentioned transition bands of HIMA with the addition of Cr^{3+} cations were shifted to 29 and 25 nm a bathochromic (red) shift. This was attributed to the inhibition of the internal charge transfer (ICT) with the addition of a Cr^{3+} ion into the HIMA solution [25].

Fluorescence Response of the Fluorescent Chemosensor

The fluorescence response of the developed chemosensor (HIMA) was studied in the presence of the stock solution of the HIMA chemosensor and different metal ions such as Al^{3+} , Ba^{2+} , Cd^{2+} , Co^{2+} , Cr^{3+} , Fe^{3+} , K^+ , Li^+ , Mn^{2+} , Ni^{2+} , Pb^{2+} , Zn^{2+} , and Zr^{4+} (Fig. 3). This measurement to recognize the selectivity of HIMA chemosensor towards cations was performed by the addition test solution of 1 mL fluorescent sensor solution (24 μM) in DMF/deionized water and 2 mL cations (72 μM) in deionized water. The developed PAMU-based chemosensor showed a strong emission band at 557 nm when excited at 497 nm, and its emission intensity was recorded as 47.442 a.u. With the addition of cations in the HIMA solution, emission intensities were measured as 15.058, 57.764, 69.914, 71.234, 83.363, 86.819, 93.935, 100.577, 106.744, 117.114, 124.772, 131.368, and 135.286 a.u. for Cr^{3+} , Mn^{2+} , Co^{2+} , Pb^{2+} , Zn^{2+} , Ba^{2+} , Li^+ , K^+ , Al^{3+} , Cd^{2+} , Fe^{3+} , Ni^{2+} , and Zr^{4+} , respectively at the mentioned wavelength. These results indicated that the emission intensity of HIMA was dramatically changed in the presence of Cr^{3+} by the quenching effect while it was increased in the presence of the other tested metal ions. This quenching effect

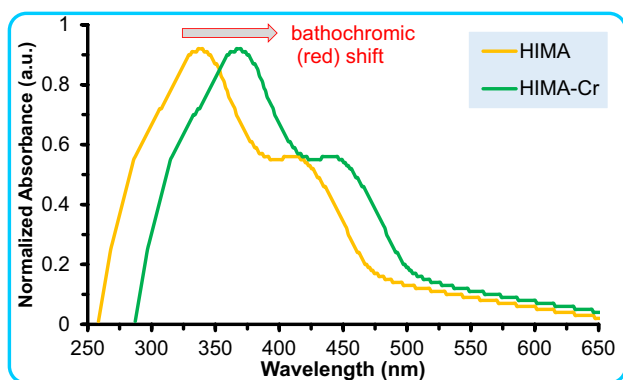


Fig. 2 UV-Vis spectra of HIMA and HIMA-Cr (Concentration: HIMA = 24 μM , Cr^{3+} = 72 μM ; $v:v = \text{HIMA}/\text{Cr}^{3+}$: 1/2 in DMF/deionized water)

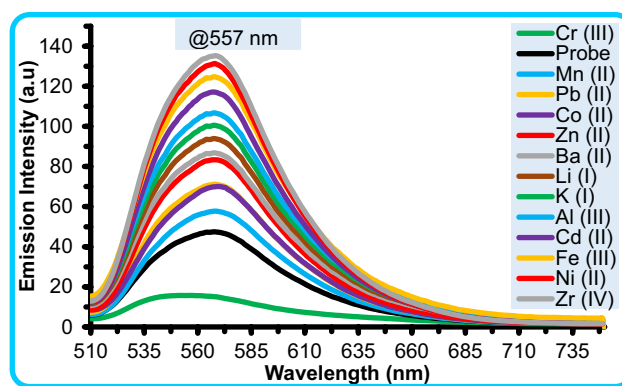


Fig. 3 Fluorescence spectra of HIMA in the presence of different concentrations of cations (Concentration: HIMA = 24 μM , metal ions = 72 μM , $v:v = \text{HIMA}/\text{cation}$: 1/2 in DMF/deionized water)

could be explained by the interaction of functional groups such as azomethine ($-\text{N}=\text{CH}$), hydroxyl ($-\text{OH}$), urethane $-\text{NH}$, and carbonyl ($-\text{C}=\text{O}$) in the structure of HIMA with Cr^{3+} ion [26].

Cr^{3+} Cation Concentrations Effect

To investigate the potential spectral efficiency and applicability of the HIMA chemosensor, its emission intensity was measured in the presence of different Cr^{3+} cation concentrations under 497 nm excitation wavelength, and at the ambient conditions (Fig. 4). Emission intensities were recorded as 48.72, 45.42, 43.04, 41.15, 38.75, 36.45, 30.25, 24.58, 15.72, and 12.24 in the presence of 2, 4, 8, 12, 16, 24, 32, 48, 64, and 72 μM of Cr^{3+} concentrations, respectively. These results revealed that the emission intensity of the HIMA chemosensor was gradually decreased with the increasing Cr^{3+} cations concentrations.

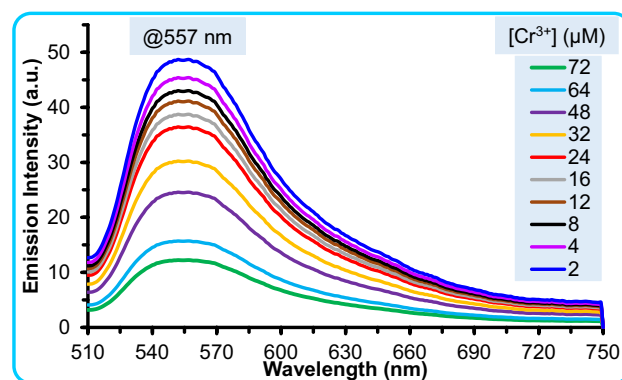


Fig. 4 Fluorescence spectra of HIMA in the presence of different Cr^{3+} concentrations (Concentration: HIMA = 24 μM , $v:v = \text{HIMA}/\text{Cr}^{3+}$: 1/2 in DMF/deionized water)

Limit of Detection (LOD) and Limit of Quantification (LOQ)

To test the practical applicability of the HIMA chemosensor, a calibration curve was obtained by plotting the emission intensities against the different chromium (III) concentrations (Fig. S1). As can be seen from the obtained calibration curve, the HIMA chemosensor showed a gradually decreasing linear response toward increasing Cr^{3+} cations concentrations. Also, this linearity value was detected as 0.9933.

The limit of detection (LOD) and the limit of quantification (LOQ) of the proposed chemosensor was calculated by using the following equations (Eqs. 1, and 2) and emission titration methods, respectively [27, 28]:

$$\text{LOD} = \frac{3 \sigma_{bi}}{m} \quad (1)$$

$$\text{LOQ} = \frac{10 \sigma_{bi}}{m} \quad (2)$$

where σ_{bi} and m are the standard deviations (0.012) of metal-free chemosensor solutions and slope ($m = 0.4964$) obtained from Fig. S1, respectively. The regression equation of HIMA in the presence of Cr^{3+} was found as $I = -0.4964[\text{Cr}^{3+}] + 47.629$. LOD and LOQ values of 7.98×10^{-8} M (0.0798 μM , 0.024 ppm), and 2.42×10^{-7} M (0.242 μM), respectively.

According to the World Health Organization (WHO) and the United States Environmental Protection Agency, the maximum amount of Cr^{3+} allowed in drinking water has been reported as 0.05 ppm (0.05 mg/L), and 0.015 ppm (0.015 mg/L), respectively [29]. As can be seen in the LOD value of the HIMA chemosensor in the presence of Cr^{3+} , it was calculated to be lower than the maximum amount in drinking water reported by WHO and USA Environmental Protection Agency.

To investigate the binding efficiency of the proposed chemosensor, the stoichiometry between HIMA chemosensor and Cr^{3+} cations was determined using Job's plot method (Fig. S2) [30]. The maximum emission intensity was obtained at the ratio $[\text{Cr}^{3+}] / ([\text{Cr}^{3+}] + [\text{HIMA}]) = 0.5$. This result showed that the host–guest interaction between HIMA chemosensor and Cr^{3+} cations was performed in a 1:1 stoichiometric ratio.

In addition, the binding constant (K_a) of the HIMA chemosensor with Cr^{3+} cations was calculated by using the following Benessi-Hildebrand equation (Eq. 3) [31]:

$$\frac{1}{I - I_0} = \frac{1}{K_a(I_{\max} - I_0)[M]} + \frac{1}{I_{\max} - I_0} \quad (3)$$

where I , I_0 , and I_{\max} are emission intensities of HIMA chemosensor with Cr^{3+} , without Cr^{3+} , and saturated solution in the presence of the maximum amount of cation, respectively. Also, $[M]$ is the concentration of added $[\text{Cr}^{3+}]$ cations. K_a value was found as $5.31 \times 10^5 \text{ M}^{-1}$. This calculated K_a value was compatible with the reported studies in the literature for the determination of trivalent cations [32, 33].

As demonstrated in Table S1, the HIMA chemosensor for the detection of Cr^{3+} cations was compared to the previously reported paper in the literature in terms of structure, LOD value, and media. It was clearly seen in the finding results that the developed chemosensor had a lower and satisfactory LOD value compared to the chemosensor in Table 1, and it was done progress in the LOD value according to the other studies.

To examine the complex interaction between the prepared HIMA chemosensor with Cr^{3+} cation, the $^1\text{H-NMR}$ titration method was used and $^1\text{H-NMR}$ spectra of HIMA in the absence and presence of Cr^{3+} cation were given in Fig. 5a. As can be seen in Fig. 5a, urethane $-\text{NH}$, hydroxyl $(-\text{OH})$, and imine $(-\text{N}=\text{CH})$ protons were detected at 9.71, 8.44, and 7.88 ppm for the HIMA, and 9.92, 8.50, and 7.95 ppm for HIMA–Cr complex. These results revealed that the proton peak values of the complex were shifted to the higher values, and they were weakened. According to these results, the possible complexation was carried out with Cr^{3+} ions between urethane, hydroxyl, and imine functional groups (Fig. 5b) [34, 35].

Interference

To investigate the performance and selectivity of the chemosensor, the possible interference effect of the tested cations (Mn^{2+} , Co^{2+} , Pb^{2+} , Zn^{2+} , Ba^{2+} , Li^+ , K^+ , Al^{3+} , Cd^{2+} , Fe^{3+} , Ni^{2+} , and Zr^{4+}) (72 μM) on the fluorescence intensity of the HIMA (24 μM) was evaluated in the presence of Cr^{3+} cations (72 μM) (Fig. 6). As represented in Fig. 6, the tested metal cations did not have any significant interference effect on the sensor developed to detect Cr^{3+} cations. This was attributed to the strong complexation between the HIMA

Table 1 Determination of Cr^{3+} cations in different water samples

Water sample	Spiked cation (μM)	Determined cation concentration (μM)	Recovery (%)	^a RSD (%)
Drinking water	20	20.23	101.15	1.89
Drinking water	50	50.47	100.94	1.77
Seawater	20	20.35	101.75	2.07
Seawater	50	50.57	101.14	1.85
Tap water	20	20.49	102.45	2.11
Tap water	50	50.63	101.26	1.93

^a RSD: The relative standard deviation

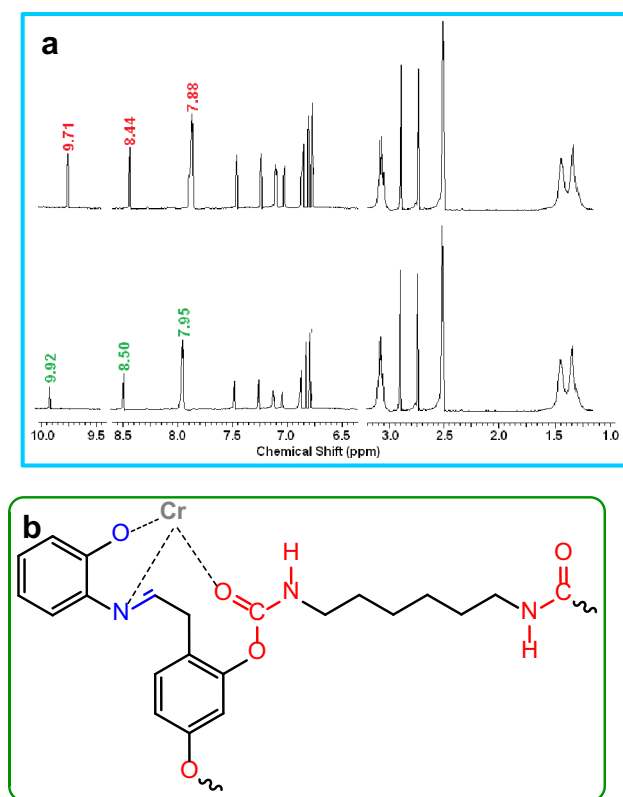


Fig. 5 $^1\text{H-NMR}$ spectra of HIMA in the absence and presence of Cr^{3+} (a), and the proposed sensing mechanism (b)

and Cr^{3+} , and the paramagnetic quenching effect of the mentioned cation due to the paramagnetic nature [36].

Reversibility

In order to test the reversibility of the developed PAMU-based fluorescent sensor, Cr^{3+} and EDTA were sequentially added to the HIMA chemosensor solution in DMF (Fig. 7). According

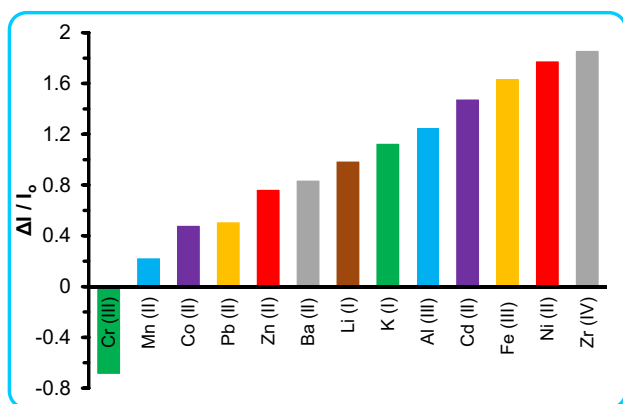


Fig. 6 Interference of different cations effect on the emission intensity of HIMA (Concentration: HIMA = 24 μM , cation = 72 μM ; $v:v = \text{HIMA}/\text{Cr}^{3+}$: 1/2 in DMF/deionized water)

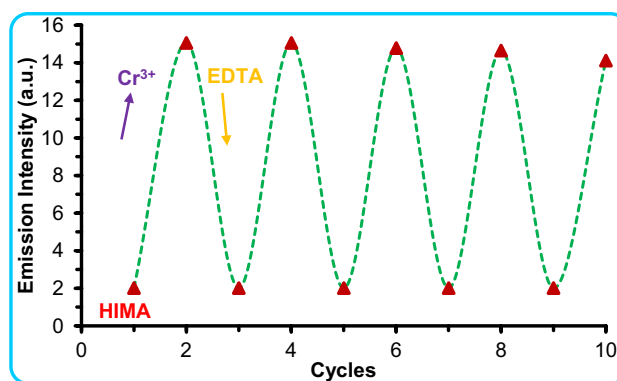


Fig. 7 Fluorescence spectra of HIMA (24 μM) after the sequential addition of Cr^{3+} (72 μM) and EDTA (72 μM)

to the results of the finding, the emission intensity of the HIMA chemosensor was slightly decreased after the 6th cycle and the sequential addition of cation and EDTA. This finding indicated that the developed PAMU-based chemosensor has been potentially applied for the determination and identification of Cr^{3+} cations as a selective and sensitive fluorescent sensor.

Photostability

Another parameter used to evaluate the efficiency of the fluorescence chemosensor is photostability. To investigate the photostability of the HIMA chemosensor, its emission intensity was measured in the presence of a 1 mL fluorescent probe and 2 mL of Cr for 60 min (Fig. 8). As can be seen in Fig. 8, HIMA lost its emission intensity value at 0.87, 2.34, 3.00, 3.55, 4.89, and 5.82% after 10, 20, 30, 40, 50, and 60 min, respectively. Also, the proposed sensor lost its emission intensity at 0.52, 2.24, 2.71, 3.37, 4.04, and 4.70% at the mentioned times. These findings indicated that the HIMA chemosensor exhibited excellent photostability.

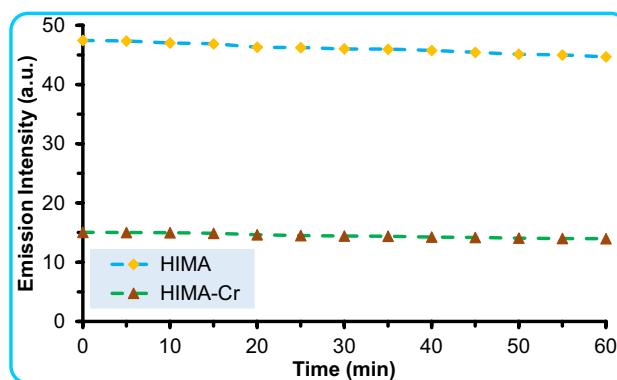


Fig. 8 Photostability of HIMA with/without Cr^{3+} (Concentration: HIMA = 24 μM , cation = 72 μM ; $v:v = \text{HIMA}/\text{Cr}^{3+}$: 1/2 in DMF/deionized water)

Real Sample Applications

To test the applicability of the HIMA chemosensor in different water samples, it was tested with Cr^{3+} fluorescence and UV–Vis measurements in the drinking, sea, and tap water samples (Table 1). Cation concentrations were found as 20.23, 20.35, and 20.49 μM in the presence of 20 μM spiked Cr^{3+} cations, and 50.47, 50.57, 50.63 μM in the presence of 20 μM spiked Cr^{3+} cations for drinking, sea, and tap water samples. Recovery and RSD values were also recorded in the range from 100.94 to 102.45%, and 1.89 to 2.11%. These results exhibited that the HIMA chemosensor was successfully applied in the determination of Cr^{3+} cations amount in the different water samples.

Conclusion

In the present paper, an effective and highly selective fluorescent chemosensor based on poly(azomethine-urethane) (HIMA) was developed for the detection of Cr^{3+} cations in different water samples. The limit of detection (LOD) and quantitation (LOQ) of the HIMA sensor were calculated as 7.98×10^{-7} , and 2.42×10^{-6} M respectively, and they were found to be lower than the maximum amount in drinking water reported by WHO and USA Environmental Protection Agency. Also, stoichiometry between the HIMA and Cr^{3+} cations was found as 1:1, and the binding constant (K_a) was calculated as $5.31 \times 10^5 \text{ M}^{-1}$. These findings indicated that the proposed HIMA chemosensor could be found to potential application for the determination of Cr^{3+} cations in different water samples with satisfying, reliable, practical, and accuracy.

Supplementary Information The online version contains supplementary material available at <https://doi.org/10.1007/s10895-022-03037-7>.

Author Contributions Musa Kamaci is the single author of this manuscript. He has solely designed the manuscript.

Funding The authors declare that no funds, grants, or other support were received during the preparation of this manuscript.

Data Availability All data generated or analyzed during this study are included in this published article.

Code Availability Not applicable.

Declarations

Ethical Approval Not applicable.

Consent to Participate Not applicable.

Consent for Publication Not applicable.

Conflict of Interest The author also declares that there is no conflict of interest.

References

- Ge Q, Feng X, Wang R, Zheng R, Luo S, Duan L, Ji Y, Lin J, Chen H (2020) Mixed redox-couple-involved chalcopyrite phase CuFeS_2 quantum dots for highly efficient Cr(VI) removal. *Environ Sci Technol* 54:8022–8031. <https://doi.org/10.1021/acs.est.0c01018>
- Chen F, Guo S, Wang Y, Ma L, Li B, Song Z, Huang L, Zhang W (2022) Concurrent adsorption and reduction of chromium(VI) to chromium(III) using nitrogen-doped porous carbon adsorbent derived from loofah sponge. *Front Environ Sci Eng* 16:57. <https://doi.org/10.1007/s11783-021-1491-6>
- Zhang X, Yang Z, Mei J, Hu Q, Chang S, Hong Q, Yang S (2022) Outstanding performance of sulfurated titanomagnemite (Fe_2TiO_5) for hexavalent chromium removal: Sulfuration promotion mechanism and its application in chromium resource recovery. *Chemosphere* 287:132360. <https://doi.org/10.1016/j.chemosphere.2021.132360>
- Yang J, Li C, Yang B, Kang S, Zhang Z (2018) Study on adsorption of chromium (VI) by activated carbon from cassava sludge. *IOP Conf Ser Earth Environ Sci* 128:012017. <https://doi.org/10.1088/1755-1315/128/1/012017>
- Yan BZ, Chen ZF (2019) Influence of pH on Cr(VI) reduction by organic reducing substances from sugarcane molasses. *Appl Water Sci* 9:61. <https://doi.org/10.1007/s13201-019-0940-x>
- Nguyen NT, Lee SY, Chen SS, Nguyen NC, Chang CT, Hsiao SS, Trang LT, Kao CY, Lin MF, Wang L (2018) Preparation of Zn doped biochar from sewage sludge for chromium ion removal. *J Nanosci Nanotechnol* 18:5520–5527. <https://doi.org/10.1166/jnn.2018.15392>
- Sangsin S, Srivilai P, Tongraung P (2021) Colorimetric detection of Cr^{3+} in dietary supplements using a smartphone based on EDTA and tannic acid-modified silver nanoparticles. *Spectrochim Acta A Mol Biomol Spectrosc* 246:119050. <https://doi.org/10.1016/j.saa.2020.119050>
- Kosla T, Lasocka I, Skibniewska EM, Kolnierzak M, Skibniewski M (2018) Trivalent chromium (Cr III) as a trace element essential for animals and humans. *Med Weter* 74:560–567. <https://doi.org/10.21521/mw.6035>
- Zarczynska K, Krzbiec S (2018) The effect of chromium on ruminant health. *J Elem* 25:893–903. <https://doi.org/10.5601/jelem.2020.25.1.1963>
- Lv Z, Tang Y, Dong S, Zhou Q, Cui G (2022) Polyurethane-based polymer electrolytes for lithium batteries: Advances and perspectives. *Chem Eng J* 430:132659. <https://doi.org/10.1016/j.cej.2021.132659>
- Cheng BX, Gao WC, Ren XM, Ouyang XY, Zhao Y, Zhao H, Wu W, Huang CX, Liu Y, Liu XY, Li HN, Li RKY (2022) A review of microphase separation of polyurethane: Characterization and applications. *Polym Test* 107:107489. <https://doi.org/10.1016/j.polymertesting.2022.107489>
- Lee DW, Kim HN, Lee DS (2018) Design of azomethine diols for efficient self-healing of strong polyurethane elastomers. *Molecules* 23:2928. <https://doi.org/10.3390/molecules23112928>
- Kamaci M, Kaya I (2016) New low-band gap polyurethanes containing azomethine bonding: Photophysical, electrochemical, thermal and morphological properties. *J Taiwan Inst Chem Eng* 59:536–546. <https://doi.org/10.1016/j.jtice.2015.08.018>

14. Kaya I, Yildirim M, Kamaci M (2011) A new kind of optical Mn(II) sensor with high selectivity: Melamine based poly(azomethine-urethane). *Synth Met* 161:2036–2040. <https://doi.org/10.1016/j.synthmet.2011.06.029>
15. Kaya I, Kamaci M (2013) Highly selective and stable fluorescent sensor for Cd(II) based on poly(azomethine-urethane). *J Fluoresc* 23:115–121. <https://doi.org/10.1007/s10895-012-1124-3>
16. Kamaci M, Kaya I (2015) The novel poly(azomethine-urethane): synthesis, morphological properties and application as a fluorescent probe for detection of Zn²⁺ ions. *J Inorg Organomet Polym* 25:1250–1259. <https://doi.org/10.1007/s10904-015-0234-1>
17. Avci A, Kaya I (2015) A new selective fluorescent sensor for Zn(II) ions based on poly(azomethine-urethane). *Tetrahedron Lett* 56:1820–1824. <https://doi.org/10.1016/j.tetlet.2015.02.079>
18. Kamaci M, Kaya I (2015) 2,4-Diamino-6-hydroxypyrimidine based poly(azomethine-urethane): synthesis and application as a fluorescent probe for detection of Cu²⁺ in aqueous solution. *J Fluoresc* 25:1339–1349. <https://doi.org/10.1007/s10895-015-1624-z>
19. Kamaci M, Kaya I (2017) A highly selective, sensitive and stable fluorescent chemosensor based on Schiff base and poly(azomethine-urethane) for Fe³⁺ ions. *J Ind Eng Chem* 46:234–243. <https://doi.org/10.1016/j.jiec.2016.10.035>
20. Kamaci M, Kaya I (2019) Polymeric fluorescent film sensor based on poly(azomethine-urethane): Ion sensing and surface properties. *React Funct Polym* 136:1–8. <https://doi.org/10.1016/j.reactfunctpolym.2018.12.021>
21. Duru Kamaci U, Kamaci M, Peksel A (2019) Poly(azomethine-urethane) and zeolite-based composite: Fluorescent biosensor for DNA detection. *Spectrochim Acta A Mol Biomol Spectrosc* 212:232–239. <https://doi.org/10.1016/j.saa.2019.01.011>
22. Kaya I, Kamaci M (2012) Novel poly(azomethine-urethane)s and their polyphenol derivatives derived from aliphatic diisocyanate compound: synthesis and thermal characterization. *J Appl Polym Sci* 125:876–887. <https://doi.org/10.1002/app.36251>
23. Kaya I, Solak E, Kamaci M (2021) Synthesis and multicolor, photophysical, thermal, and conductivity properties of poly(imine)s. *J Taiwan Inst Chem Eng* 123:328–337. <https://doi.org/10.1016/j.jtice.2021.05.010>
24. Kamaci M, Kaya I (2014) Photophysical, electrochemical, thermal and morphological properties of polyurethanes containing azomethine bonding. *J Macromol Sci A* 51:805–819. <https://doi.org/10.1080/10601325.2014.937129>
25. Kolcu F, Erdener D, Kaya I (2021) Synthesis and characterization of a highly selective turn-on fluorescent chemosensor for Sn²⁺ derived from diimine Schiff base. *Synthetic Met* 272:116668. <https://doi.org/10.1016/j.synthmet.2020.116668>
26. Feng E, Fan C, Wang N, Liu G, Pu S (2018) A highly selective diarylethene chemosensor for colorimetric detection of CN⁻ and fluorescent relay-detection of Al³⁺/Cr³⁺. *Dyes Pigm* 151:22–27. <https://doi.org/10.1016/j.dyepig.2017.12.041>
27. Duru Kamaci U, Kamaci M, Peksel A (2021) A dual responsive colorimetric sensor based on polyazomethine and ascorbic acid for the detection of Al (III) and Fe (II) ions. *Spectrochim Acta A Mol Biomol Spectrosc* 254:119650. <https://doi.org/10.1016/j.saa.2021.119650>
28. Shrivastava A, Gupta VB (2011) Methods for the determination of limit of detection and limit of quantitation of the analytical methods. *Chron Young Sci* 2:21–25. <https://doi.org/10.4103/2229-5186.79345>
29. Jofre LG, Cepeda RIC (2016) Effects of Cr³⁺ ions on electrophysiological parameters of isolated skin of toad *Pleurodema thaul*. *J Adv Pharm Technol Res* 7:87–90. <https://doi.org/10.4103/2231-4040.184587>
30. Mohanasundaram D, Bhaskar R, Lenin N, Nehru K, Rajagopal G, Kumar GGV, Rajesh J (2022) A simple triphenylamine based turn-off fluorescent sensor for copper (II) ion detection in semi-aqueous solutions. *J Photochem Photobiol A* 427:113850. <https://doi.org/10.1016/j.jphotochem.2022.113850>
31. Chalmardi GB, Tajbakhsh M, Hasani N, Bekhradnia A (2018) A new Schiff-base as fluorescent chemosensor for selective detection of Cr³⁺: An experimental and theoretical study. *Tetrahedron* 74:2251–2260. <https://doi.org/10.1016/j.tet.2018.03.046>
32. Paul S, Goswami S, Manna A (2015) A differentially selective molecular probe for detection of trivalent ions (Al³⁺, Cr³⁺ and Fe³⁺) upon single excitation in mixed aqueous medium. *Dalton Trans* 44:11805–11810. <https://doi.org/10.1039/C5DT01314C>
33. Mehata MS (2021) An efficient excited-state proton transfer fluorescence quenching based probe (7-hydroxyquinoline) for sensing trivalent cations in aqueous environment. *J Mol Liq* 326:115379. <https://doi.org/10.1016/j.molliq.2021.115379>
34. Hu T, Wang L, Li J, Zhao Y, Cheng J, Li W, Chang Z, Sun C (2021) A new fluorescent sensor L based on fluorene-naphthalene Schiff base for recognition of Al³⁺ and Cr³⁺. *Inorg Chim Acta* 524:120421. <https://doi.org/10.1016/j.ica.2021.120421>
35. Krishnan U, Iyer SK (2022) Iminothiophenol Schiff base-based fluorescent probe for dual detection of Hg²⁺ and Cr³⁺ ions and its application in real sample analysis. *J Photochem Photobiol A Chem* 425:113663. <https://doi.org/10.1016/j.jphotochem.2021.113663>
36. Das B, Ghosh A, Dorairaj DP, Dolai M, Karvemu R, Mabhai S, Im H, Dey S, Jana A, Misra A (2022) Multiple ion (Al³⁺, Cr³⁺, Fe³⁺, and Cu²⁺) sensing using a cell-compatible rhodamine-phenolphthalein-derived Schiff-base probe. *J Mol Liq* 354:118824. <https://doi.org/10.1016/j.molliq.2022.118824>

Publisher's Note Springer Nature remains neutral with regard to jurisdictional claims in published maps and institutional affiliations.

Springer Nature or its licensor holds exclusive rights to this article under a publishing agreement with the author(s) or other rightsholder(s); author self-archiving of the accepted manuscript version of this article is solely governed by the terms of such publishing agreement and applicable law.